

# Human 21T breast epithelial cell lines mimic breast cancer progression *in vivo* and *in vitro* and show stage-specific gene expression patterns

Lesley H Souter<sup>1,2</sup>, Joseph D Andrews<sup>1</sup>, Guihua Zhang<sup>1</sup>, Amy C Cook<sup>1,2</sup>, Carl O Postenka<sup>1</sup>, Waleed Al-Katib<sup>1,7</sup>, Hon S Leong<sup>1</sup>, David I Rodenhiser<sup>1,3,4,5</sup>, Ann F Chambers<sup>1,2,6</sup> and Alan B Tuck<sup>1,2,6</sup>

Early breast cancer progression involves advancement through specific morphological stages including atypical ductal hyperplasia (ADH), ductal carcinoma *in situ* (DCIS) and invasive mammary carcinoma (IMC), although not necessarily always in a linear fashion. Observational studies have examined genetic, epigenetic and gene expression differences in breast tissues representing these stages of progression, but model systems which would allow for experimental testing of specific factors influencing transition through these stages are scarce. The 21T series cell lines, all originally derived from the same patient with metastatic breast cancer, have been proposed to represent a mammary tumor progression series. We report here that three of the 21T cell lines indeed mimic specific stages of human breast cancer progression (21PT-derived cells, ADH; 21NT-derived cells, DCIS; 21MT-1 cells, IMC) when grown in the mammary fat pad of nude mice, albeit after a year. To develop a more rapid, readily manipulatable *in vitro* assay for examining the biological differences between these cell lines, we have used a 3D Matrigel system. When the three cell lines were grown in 3D Matrigel, they showed characteristic morphologies, in which quantifiable aspects of stage-specific *in vivo* behaviors (ie, differences in acinar structure formation, cell polarization, colony morphology, cell proliferation, cell invasion) were recapitulated in a reproducible fashion. Gene expression profiling revealed a characteristic pattern for each of the three cell lines. Interestingly, Wnt pathway alterations are particularly predominant in the early transition from 21PTci (ADH) to 21NTci (DCIS), whereas alterations in expression of genes associated with control of cell motility and invasion phenomena are more prominent in the later transition of 21NTci (DCIS) to 21MT-1 (IMC). This system thus reveals potential therapeutic targets and will provide a means of testing the influences of identified genes on transitions between these stages of pre-malignant to malignant growth.

*Laboratory Investigation* (2010) 90, 1247–1258; doi:10.1038/labinvest.2010.97; published online 10 May 2010

**KEYWORDS:** breast cancer; tumor progression; expression microarray; atypical ductal hyperplasia; ductal carcinoma *in situ*; invasive mammary carcinoma

Pathological and epidemiological evidence has led to a histological model of breast cancer evolution, in which stem cells from the terminal duct lobular unit give rise to atypical ductal hyperplasia (ADH) or atypical lobular hyperplasia, which can then progress to ductal carcinoma *in situ* (DCIS) or lobular carcinoma *in situ*, respectively, and eventually to invasive mammary carcinomas (IMC).<sup>1–6</sup> These histological patterns are, however, most likely only rough

phenotypic indications of underlying cellular and molecular events determining progression,<sup>7</sup> and may not necessarily occur in a linear fashion. There is currently much interest in identifying the nature of the cellular and molecular events involved, not only for use in determining at which point a lesion is most likely to progress to malignancy, but also in hopes of finding a way to halt progression at these early stages.

<sup>1</sup>London Regional Cancer Program, London Health Sciences Centre, London, Ontario, Canada; <sup>2</sup>Department of Pathology, The University of Western Ontario, London, Ontario, Canada; <sup>3</sup>Department of Biochemistry, The University of Western Ontario, London, Ontario, Canada; <sup>4</sup>Department of Paediatrics, The University of Western Ontario, London, Ontario, Canada; <sup>5</sup>Children's Health Research Institute, London, Ontario, Canada and <sup>6</sup>Department of Oncology, The University of Western Ontario, London, Ontario, Canada

Correspondence: Dr AB Tuck, MD, PhD, Department of Pathology, London Health Sciences Centre, University Hospital, 339 Windermere Road, London, ON, Canada N6A 5A5.

E-mail: atuck@uwo.ca

<sup>7</sup>Current address: Faculty of Pharmacy, Al-Zytoonah Private University of Jordan, Amman, Jordan.

Received 11 December 2009; revised 4 February 2010; accepted 9 March 2010

Microarray technology and proteomics have identified candidate genes with potential involvement in cell proliferation, cell death, cell adhesion, migration, invasion, etc., at different stages of breast cancer progression.<sup>8–13</sup> Although providing important information concerning gene expression between samples at any given stage of progression, this is only a static representation of what is presumed to be a dynamic process. Model systems are thus needed, in addition to histological analysis of human breast specimens, to directly evaluate the effects of expression of specific genes, to determine the functional roles of these genes at different stages of tumor progression.

There have been a number of different approaches to modeling early breast cancer progression. Some have made use of murine models whereby premalignant lesions are induced by viral, chemical, or hormonal agents (reviewed in Medina<sup>14</sup>), or whereby genetically engineered mice are generated, which are susceptible to developing mammary epithelial neoplasia or preneoplasia (reviewed in Cardiff *et al*<sup>15</sup>). In these instances, it is mouse-derived pre-malignant lesions that are being generated and studied, which show both similarities and differences with their human counterparts. Other models have used human breast epithelial cell lines that have been spontaneously transformed, transduced with oncogenic viruses, or transfected with activated oncogenes to derive altered cells that mimic premalignant lesions when tested in immune deficient rodent hosts (eg, HMT-3522 and MCF10AT series, reviews in Weaver *et al*, Miller, Stampfer *et al*, Santner *et al*, Briand and Lykkesfeldt<sup>16–20</sup>). These systems are useful, but suffer the disadvantages of lack of representation of earlier (pre-DCIS) stages of progression (HMT-3522 series), the presence of mixed phenotypes, lack of stability of the phenotypes after culture (both series), or the dependence on *ras* transformation (MCF10AT series).

For ease of experimental manipulation, there has been much interest in comparing cells of premalignant and malignant status in 3D *in vitro* cultures.<sup>21–27</sup> By allowing cells to grow in 3D conformation in extracellular matrix certain characteristics of cell morphogenesis, proliferation, apoptosis and invasiveness may be studied in a controlled system. Using such 3D culture systems, much information has been generated on the molecular controls of morphogenesis in breast epithelial cells of different origins.<sup>21–23,28–35</sup> To this point however, only limited use has been made of such 3D *in vitro* systems to directly model aspects of early breast cancer progression.

The 21T series cell lines, which were derived from a single patient with metastatic breast cancer, have been proposed to represent a human breast cancer progression series.<sup>36</sup> The 21PT and 21NT cell lines were established from the mastectomy specimen and have been found to be stably non-tumorigenic, and tumorigenic but non-metastatic, respectively, in nude mice.<sup>36</sup> The third cell line, 21MT-1, was derived from a malignant pleural effusion and has been

found to be both tumorigenic and metastatic.<sup>36</sup> 21T series cells all express cytokeratins 8, 18 and 19, as well as HMFG-2,<sup>36</sup> identifying them as epithelial cells of mammary origin. Although all three cell lines were initially thought to be ER and PR negative, subsequent work showed the 21PT cell line to express a variant ER-receptor, which is not well detected by conventional anti-ER antibodies.<sup>37,38</sup>

To further explore the potential of the 21T series human breast cell lines as a functional model of early breast cancer progression, we have investigated their behavior both histologically *in vivo* and in 3D *in vitro* cultures. Characterization of these cells at the molecular level, using gene expression profiling of cells grown in 3D culture revealed stage-specific differences in genes involved in certain signaling pathways and functional categories reflective of progression to a more aggressive phenotype. Comparison with published microarray data from clinical human specimens has generated a 'genes of interest' short list, consisting of genes, which have potential clinical relevance and are thus prime candidates for further functional testing and development as stage-specific targets to block breast cancer progression.

## MATERIALS AND METHODS

### Cell Lines and Culture

The 21T series cell lines (21PT, 21NT, 21MT-1) were obtained as a kind gift of Dr Vimla Band (Dana Farber Cancer Institute).<sup>36</sup> These cells were maintained in culture in  $\alpha$ -MEM supplemented with 10% fetal bovine serum (FBS), 2 mM L-glutamine (both from Gibco Life Technologies, Grand Island, NY, USA), insulin (1 mg/ml), epidermal growth factor (12.5 ng/ml), hydrocortisone (2.8 mM), 10 mM 4-(2-hydroxyethyl)-1-piperazineethanesulfonic acid (HEPES), 1 mM sodium pyruvate, 0.1 mM non-essential amino acids and 50 mg/mL gentamycin reagent (all from Sigma Chemical, St Louis, MO, USA), as previously described.<sup>39</sup> After addition of all reagents, this growth medium was referred to as  $\alpha$ HE. The 21PT and 21NT-derived cell lines used in this work, designated 21PTci and 21NTci, contain an empty neo-selection vector and have been used as control cell lines for previous work in our laboratory.<sup>40</sup> Culture medium for these cell lines is the same as for the parental cell lines, with the addition of 0.2 mg/ml G418 as a selection marker (Gibco Life Technologies).

### In Vivo Studies

Female athymic NCr nude mice (*nu/nu*) were housed and cared for in accordance with the recommendations of the Canadian Council on Animal Care, under a protocol approved by the University of Western Ontario Council on Animal Care. Cell lines were grown in 150 mm tissue culture dishes to ~80% confluency (log phase of growth). The cells were gently trypsinized, washed twice with sterile PBS, and resuspended in serum-free  $\alpha$ HE media at a concentration of  $1 \times 10^7$  cells per 100  $\mu$ l. Cells were injected into the second thoracic mammary fat pad of 8- to 9-week-old female nude

mice, as described elsewhere.<sup>41</sup> Animals were routinely monitored for health and primary tumors, when palpable, were measured every 7–14 days. Animals were euthanized early if the tumor burden became too great, or at the end point of the experiment (1 year post-injection). Animals were killed and necropsies performed, examining the injected mammary fat pad, locoregional lymph nodes, and all major viscera, whether or not a palpable lesion was present. Tissues were formalin-fixed, paraffin-embedded, sectioned (4  $\mu$ m thick) and examined histologically by hematoxylin and eosin (H&E) staining.

### 3D *In Vitro* Cultures

For all 3D cultures, cells were grown in Matrigel Basement Membrane Matrix (BD Biosciences, Mississauga, ON, USA) for 9 or 15 days. Cultures were created in 48-well plates (Nunc Brand Products, Rochester, NY, USA) with three distinct layers. The bottom layer consisted of undiluted Matrigel for a solid base. The middle layer contained a 1:1 mix of Matrigel and  $2 \times 10^5$  cells in media supplemented with 0.1% bovine serum albumin (BSA), instead of FBS. These two layers were topped with growth media supplemented with 0.1% BSA (without FBS). After growth in Matrigel, 10% neutral-buffered formalin was added to the dishes for 48 h and the cultures were removed as intact Matrigel plugs. The formalin-fixed plugs were then processed, paraffin-embedded and sectioned for H&E staining and immunohistochemistry.

### Morphological Characterization of 3D *In Vitro* Cultures

Histomorphology was determined by examination of 4  $\mu$ m, H&E-stained sections of the Matrigel plugs. Characterization of behavior included assessment of extracellular lumen formation, number of groups with polarized cells, spherical (*vs* non-spherical) colony formation and proportion of single cells. Each of these parameters was assessed in terms of a percentage of total ‘events’ counted.

### Proliferation and Apoptosis in 3D Culture

The 21T series cell lines were grown in Matrigel for 9 or 15 days. Matrigel plugs were immunostained for the proliferation marker, Ki67, and for the apoptotic marker, caspase 3. For caspase 3 immunohistochemistry, deparaffinized sections were pretreated in a microwave oven for epitope retrieval. Caspase 3 antibody (Cell Signaling Technologies, Danvers, MA, USA) was applied (1/300 dilution) for 15 min at room temperature. Ki67 staining was performed following a previously published protocol<sup>42</sup> with Ki67 antibody (Dako, Mississauga, ON, USA) applied (1/150 dilution) overnight at 4°C. For both caspase 3 and Ki67, detection was performed with the UltraVision LP Detection System HRP Polymer (Thermo Scientific, Waltham, MA, USA) kit, following the manufacturer’s protocol. Slides were counterstained with Harris’s Hematoxylin. Positive and negative controls were included. For each cell line, the Ki67 and caspase 3 indices,

defined as the number of cells positive for Ki67 or caspase 3 staining divided by the total cells counted, were calculated from examination of 10 high power ( $\times 400$ ) fields of view from three replicate Matrigel plugs per cell line. To determine the balance of dividing cells *vs* apoptosing cells, the ratio of proliferation over apoptosis was calculated for each cell line.

### Matrigel Invasion Assay

21T series cell lines were grown in Matrigel for 9 days in 8-well chamber slides (Nunc Brand Products). Matrigel cultures were formed as above, with adjustment made in volumes of the three layers for the smaller 8-well chamber slide.  $1.5 \times 10^4$  cells were used in the middle layer. Slides were then moved to an incubated stage platform of a Zeiss Axiovert 200 M microscope for time lapse photography. Z-stack microscopy images at 5 positions were taken for each cell line every 12 h until day 15 of growth. All cells found within the 5 positions per cell line were then followed using AxioVision 4.5 software (Carl Zeiss Imaging Solutions) to determine the percentage of cells that invaded through the Matrigel matrix and the distance the cells traveled.

### Gene Expression Profiling in 3D Culture

For expression profiling in 3D culture, cells were grown in Matrigel for 9 days in 24-well plates (Nunc Brand Products). Matrigel cultures were formed as above with an adjustment made in volumes of the three layers for the larger 24-well plate volume. Three wells per cell line, representing three biological replicates were grown. Total RNA from each biological replicate was isolated using Cell Recovery Solution (BD Biosciences) to non-enzymatically dissociate the Matrigel, followed by TRIzol (Invitrogen International, Mississauga, ON, USA), as per the manufacturer’s instructions. RNA (10  $\mu$ g) was then sent to the London Regional Genomics Centre (www.lrgc.ca, London, ON, Canada) and was used to produce Biotin-labeled cRNA, which was hybridized to Affymetrix HGU133\_Plus\_2 arrays (Affymetrix Inc., Santa Clara, CA, USA). Washing, scanning and probe quantification were carried out according to the manufacturer’s instructions, using GeneChip Operating Software (GCOS, www.affymetrix.com), with target intensity set to 150. For each array, GCOS output was imported as .txt files into Genespring GX 7.3 software (Agilent Technologies, Santa Clara, CA, USA) and data were normalized as follows: Values  $< 0.01$  were set to 0.01 and the median intensity of each array was normalized to the 50th percentile of all arrays. Finally, the intensity of each probe set in each of the three 21NTci or 21MT-1 arrays was divided by the normalized mean intensity of that probe set in the appropriate control arrays. The geometric mean of these three ratios is reported. To control the family-wise error rate, two separate analyses were performed: 21NTci *vs* 21PTci, with 21PTi as control, and 21MT-1 *vs* 21NTci, with 21NTci as control. After normalization, the data were first prefiltered. Any probe set flagged ‘absent’ by GCOS software in all nine arrays was removed from further

consideration. Next, any remaining probe set not changing at least 1.5-fold in 21NTci relative to 21PTci, or 21MT-1 relative to 21NTci was removed. Probe sets passing these criteria were analyzed using the Student's *t*-test tool in Genespring, with the nominal *P*-value set at  $P < 0.05$ . This resulted in a list of genes significantly changing in 21NTci vs 21PTci, or 21MT-1 vs 21NTci (data series GSE18370, <http://www.ncbi.nlm.nih.gov/geo/>). Genes differentially expressed between 21PTci and 21MT-1 were also examined (data not shown). To focus our search to genes relevant in a clinical setting, the 'significantly altered' gene lists were then compared with gene expression profiling information on clinically relevant databases we established from the literature related to early progression, invasion/metastasis and prognosis of breast cancer<sup>11-13,43-51</sup> (Supplementary Table 1). New genes lists created from gene expression alterations in common with the clinical databases (Supplementary Table 2) were imported into Ingenuity Pathways Analysis (IPA) (Ingenuity Systems, [www.ingenuity.com](http://www.ingenuity.com)). Each gene identifier in the data sets was mapped to its corresponding gene in the ingenuity pathways knowledge base, and if present, was considered for analysis. Functional analysis identified biological functions and/or diseases that were most significant to the data set. Canonical pathway analysis identified pathways from the IPA library that were most significant to the data set.

#### Quantitative Real Time-PCR (qRT-PCR) Validation

Total RNA was extracted from four biological replicates of each cell line following 9 days of growth in 3D Matrigel, using the same methodology employed for gene expression profiling. cDNA was synthesized from 1  $\mu$ g total RNA using Superscript II (Invitrogen International), with random primers (Invitrogen International), as per the manufacturer's instructions. qRT-PCR was performed using a Rotor-Gene RG-3000 (Corbett Life Science, San Francisco, CA, USA), in combination with SYBR-Green. RT2 qPCR primers for the selected targets (BAX, CCL20, CCR1, CDH1, CXCR4, DCN, MAX, MCM4, MGA, S100A2, S100A3, SERPINB5, SNAI2, TBX3, TFF2, TNFAIP3, VANGL1, WISP1, WNT5A) and RT2 SYBR-Green qPCR Master Mix were purchased from SuperArray Bioscience Corporation. 18S rRNA was used as an endogenous control (SuperArray Biosciences Corporation). Genes were considered to be validated if the qRT-PCR results showed statistically significant expression alterations in the same direction as the microarray.

#### Statistical Analysis

The differences between experimental groups were analyzed using one-way analysis of variance (ANOVA), followed by Tukey's test for *post hoc* analysis. For the Matrigel invasion assay, a Kruskal-Wallis nonparametric ANOVA was used when calculating the percent of cells that moved, as the values were not normally distributed. This was also followed by a Tukey's *post hoc* test. For all statistics, a *P*-value of less than 0.05 was considered statistically significant.

## RESULTS

### *In Vivo* Cultures of 21T Series Cell Lines Model Stages of Early Progression

Mice injected in the mammary fat pad with each of the three 21T series cell lines were monitored for tumor growth for up to a year. This study confirmed the previously published findings of Band *et al.*<sup>36</sup> that 21PT-derived cells are non-tumorigenic and non-metastatic, 21NT-derived cells are tumorigenic but non-metastatic, and 21MT-1 cells are tumorigenic and metastatic in some mice (Table 1). In addition, in our study, systematic histological examination of the mammary fat pads of all animals, whether or not tumors were palpable, was performed at end-point and provided some very novel information. Where microscopically discernible lesions formed, each of the injected cell lines gave rise to a characteristic histomorphology. Mammary fat pads of 21PTci-injected mice showed scattered ducts with features of ADH (Table 1 and Figure 1a). In keeping with ADH,<sup>5</sup> involved ducts of these animals showed a mixture of two epithelial cell populations, one atypical/neoplastic appearing (non-high grade), and the other normal/benign appearing (Figure 1a inset). None of the ducts in 21PTci-injected mice displayed a morphology that met criteria for DCIS (incomplete duct filling by atypical cell population, <2.0 mm in greatest extent). In contrast, mammary fat pads of 21NTci-injected mice showed a pattern of DCIS (intermediate and high nuclear grade, solid and cribriform, with zonal necrosis), which in 6/7 of those mice forming lesions had no associated invasive component (Table 1 and Figure 1b). In the one 21NTci-injected animal, in which associated invasive carcinoma was present, the degree of invasion was minimal, and no metastases were seen (Table 1). In sharp contrast to both, mammary fat pads of 21MT-1-injected mice showed a pattern of IMC in all instances where a histologically discernible lesion formed, and half of these were also associated with pulmonary metastases (Table 1 and Figure 1c). The *in vivo* growth characteristics of these three 21T series cell lines thus reproducibly model distinct histological stages of early breast progression, from ADH (21PTci) to DCIS (21NTci) to IMC (21MT-1), up to 1 year after mammary fat pad injection in mice.

**Table 1 Histopathology of 21T series cell lines *in vivo* 1 year after orthotopic mammary fat pad injection into 6- to 8-week-old female nude mice**

	No. of mice showing ADH only	No. of mice showing DCIS only	No. of mice showing invasive carcinoma	No. of mice showing metastases
21PTci	2/32	0/32	0/32	0/32
21NTci	0/29	6/29	1/29	0/29
21MT-1	0/15	0/15	10/15	5/15

ADH, atypical ductal hyperplasia; DCIS, ductal carcinoma *in situ*.

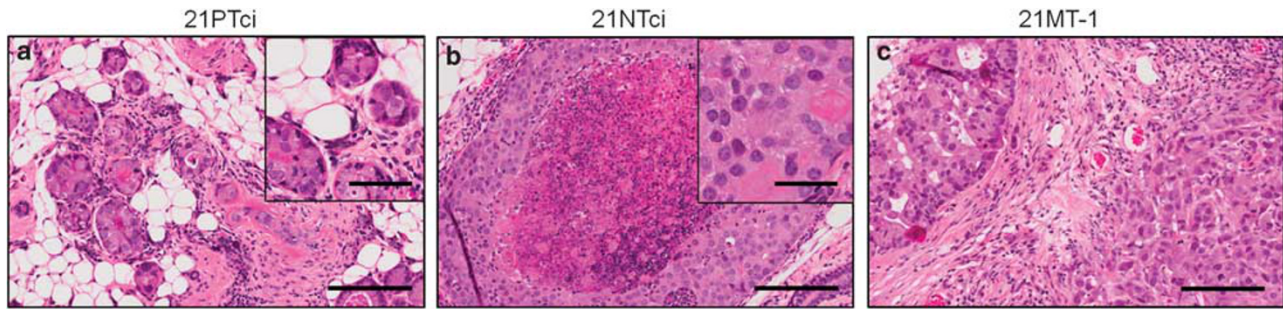


**Figure 1** Histopathology of 21T series cells *in vivo*, 1 year after injection of  $1 \times 10^7$  cells into the mammary fat pad of 6- to 8-week-old female nude mice. Histology was analyzed for mammary fat pads of all mice injected. (a) 21PTci cells mimicked aspects of ADH, with both atypical (non-high grade) and normal-appearing populations visible in a given involved duct/ductule and with the atypical cell population represented over an area of  $<2.0$  mm (ie, not meeting pathological criteria for DCIS). (b) 21NTci cell morphology mimicked DCIS, with the neoplastic cells filling an entire mammary fat pad duct, often with accompanying central zonal necrosis. This pattern was seen in multiple duct cross-sections (over an area  $>2.0$  mm). (c) 21MT-1 cells displayed a histology of IMC (no special type, SBR Grade III/III), associated with a background DCIS. All sections are H&E stained. Scale bars represent  $200 \mu\text{m}$ , except for the inset of (a and b), which represents  $100 \mu\text{m}$ . All images are 24-bit resolution TIFFs (1.8 MP) captured with an Aperio Scanscope, scanning with the  $\times 400$  objective.

### 3D *In Vitro* Cultures of 21T Series Cells Display Features of Specific Stages of Early Progression

To develop a more rapid, readily manipulatable *in vitro* system for assessing the biological differences between these cells, we made use of a 3D Matrigel model. Cells were grown in 3D Matrigel plugs for 9 or 15 days, and characterized using a number of morphological and functional parameters, including colony profile (spherical *vs* irregular), lumen formation, cell polarization, proportion of single cells, Ki67 proliferation index, caspase 3 apoptosis index and cell invasion (by time lapse microscopy). By day 15, 21PTci cells were found to form many spherical colonies, which had a high proportion of polarized cells and extracellular lumen formation (Figure 2a, d and g). Interestingly, many of the 21PTci cell colonies had an admixture of cells with nuclei that appeared either normal or atypical in morphology. In contrast, 21NTci cells showed fewer spherical colony profiles, and a lesser degree of cell polarization and lumen formation than the 21PTci cells (Figure 2b, e and g). Most of the 21NTci cell groups showed significant nuclear atypia. Finally, 21MT-1 cells showed a much lower proportion of spherical colonies (more were of irregular profile) and a high proportion of single cells than either of the other lines. In addition, 21MT-1 cell groups show even less polarization and extracellular lumen formation than 21NTci cells (Figure 2c, f and g).

### Differential Proliferation, Apoptosis and Invasiveness of 21T Series Cells

Assessment of proliferative rates by Ki67 immunohistochemistry showed that at day 9, 21NTci cells showed significantly more proliferative events than 21PTci or 21MT-1 cells ( $P < 0.01$ ) (Figure 3a). However, the proliferative rate of both 21NTci and 21PTci had dropped off by 15 days of growth in Matrigel, whereas that of 21MT-1 cells was highest at day 15 ( $3 \times$  that of 21PTci,  $P < 0.01$ ) (Figure 3a). Apop-

otic rates by caspase 3 immunohistochemistry showed that there was no significant difference between cell lines at day 9, however by day 15, apoptotic rates drop slightly and not significantly for 21PTci cells and slightly and significantly ( $P < 0.01$ ) for 21MT-1 cells (Figure 3b). The ratios of proliferation/apoptosis were calculated for the 21T series cell lines grown in Matrigel, using Ki67 (proliferation) *vs* caspase 3 (apoptosis) index. Results indicate that at day 9, 21NTci cells had the highest ratio of proliferation/apoptosis, compared with 21PTci cells ( $P < 0.05$ ) or 21MT-1 cells ( $P < 0.05$ ) (Figure 3c). However, by day 15, 21MT-1 cells showed an increased proliferation/apoptosis ratio, which was higher than either of the other 2 cell lines ( $P < 0.01$  compared with 21PTci and 21NTci) (Figure 3c). The 21NTci cells, which showed a high rate of growth at day 9, had a significantly decreased ( $P < 0.05$ ) ratio on day 15 (Figure 3c). The 21PTci cells showed a trend towards a decrease in proliferation/apoptosis at day 15 compared with day 9, but this was not significant. Interestingly, by day 15 (*vs* day 9), a higher proportion of 21PTci and 21NTci cells were present as polarized groups showing extracellular lumen formation, suggesting that the decrease in ratio of cell proliferation/apoptosis may be related to increased differentiation (data not shown), whereas the 21MT-1 showed very little polarization/extracellular lumen formation and instead showed increased growth between day 9 and day 15 (cf Figures 2 and 3).

Finally, to assess invasive ability, cells were grown in Matrigel for 9 days and then followed with time lapse microscopy until day 15. It was found that 100% of 21MT-1 cells were able to travel through the Matrigel in both horizontal and vertical directions, compared with only 25% of 21PTci and 30% of 21NTci cells (Figure 4a). In addition, 21MT-1 cells traveled  $219 \mu\text{m}$  on average over the 7 days, which was significantly ( $P < 0.01$ ) farther than that for 21PTci ( $22 \mu\text{m}$ ) and 21NTci ( $18 \mu\text{m}$ ) cells (Figure 4b).



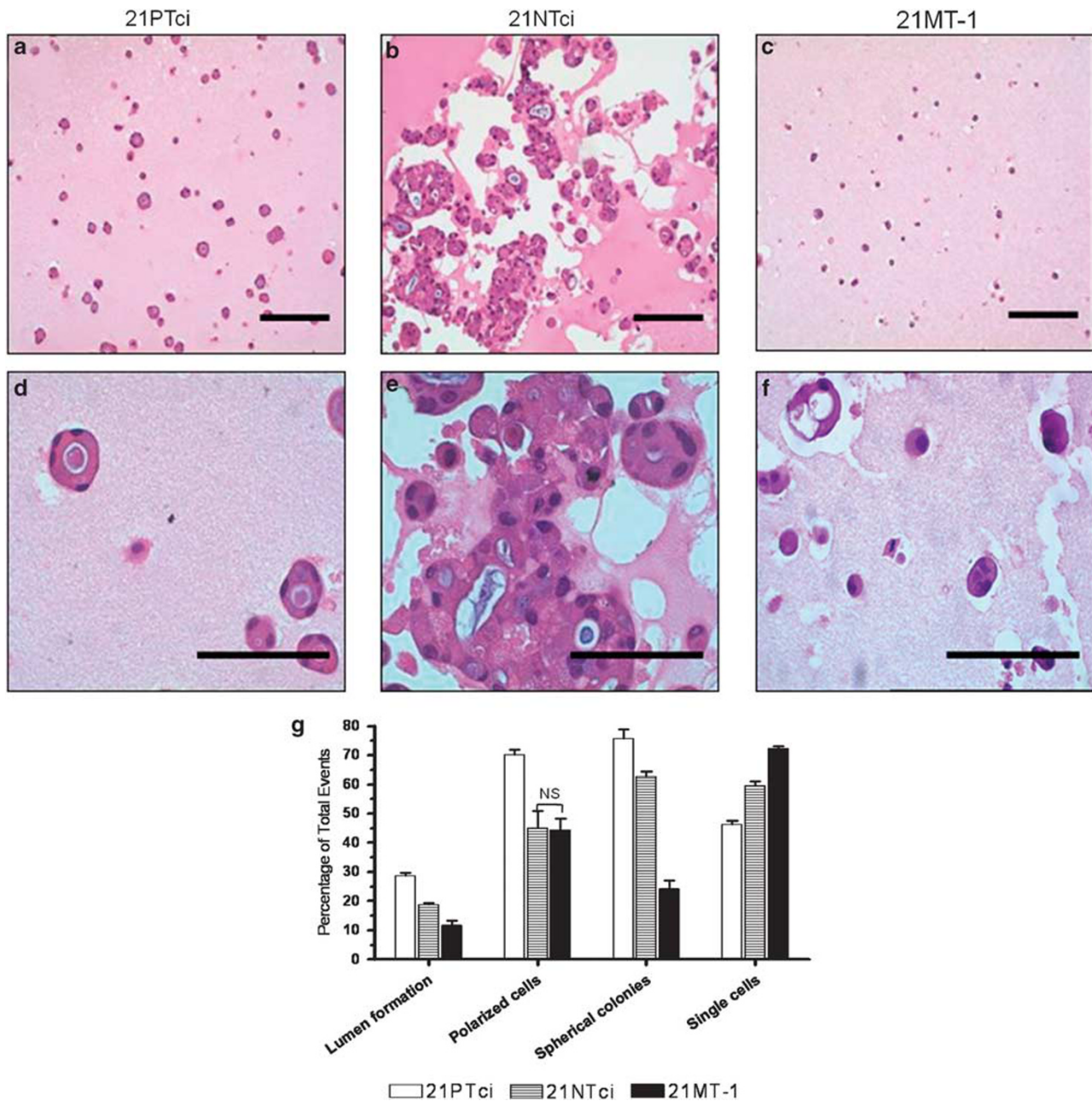


**Figure 2** *In vitro* characteristics of 21PTci, 21NTci and 21MT-1 cells after 15 days growth in 3D Matrigel. 21PTci cells (**a, d, g**) formed more polarized cell groups than 21NTci ( $P < 0.05$ ) or 21MT-1 ( $P < 0.05$ ) cells, with higher frequency of extra-cellular lumen formation ( $P < 0.01$  and  $P < 0.001$  respectively) and more crisply defined spherical colonies than 21NTci ( $P < 0.05$ ) or 21MT-1 ( $P < 0.001$ ) cells. 21NTci cells (**b, e, g**) formed large numbers of cohesive spherical colonies (~38% more compared to 21MT-1 cells,  $P < 0.001$ ), but have less tendency towards cell polarization. 21MT-1 cells (**c, f, g**) were present more as single cells (~26% more than 21PTci cells,  $P < 0.001$  and ~13% more than 21NTci cells,  $P < 0.001$ ) and small groups, which were non-spherical and less polarized (than 21PTci), in an invasive pattern of distribution. All sections are H&E stained. Images were chosen to show structures of 3D cell colonies and not typical cell density within a Matrigel plug. In (**g**) for 'single cells', an 'event' is either a single cell or a cell group/colony, whereas for the 'spherical colonies', 'lumen formation' and 'polarized cells' comparisons, an 'event' was defined as a cell group/colony. Also for (**g**) all bars within each group are significantly different from each other at a  $P$ -value of at least  $< 0.05$ , except when indicated by NS (non significant). Scale bars for (**a-c**) represent  $100 \mu\text{m}$ , whereas scale bars for (**d-f**) represent  $50 \mu\text{m}$ .

Although the majority of 21MT-1 cells that moved showed individual translational cell movement, 21PTci and 21NTci cell movement predominantly involved localized arrangement into cell groups within a confined area.

### Profiling Elucidates Differential Gene Expression between the Three 21T Series Cell Lines Grown in 3D

To determine differential gene profiles between the 21T series cell lines, 3D *in vitro* microarray expression arrays were

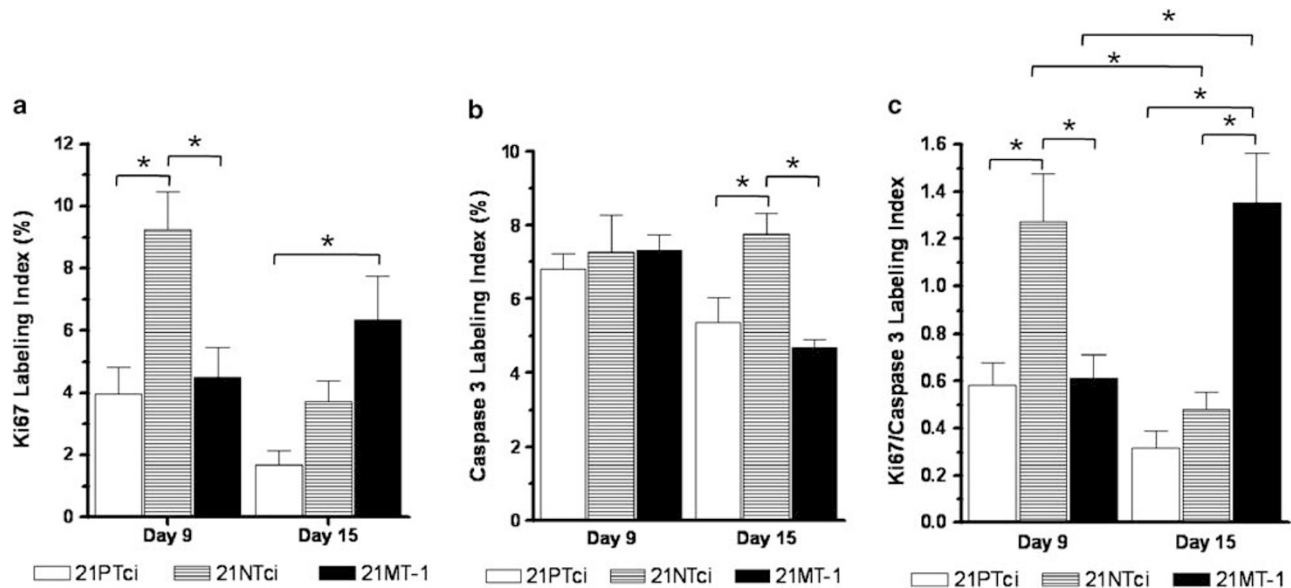


**Figure 3** Proliferative and apoptotic activity of 21PTci, 21NTci and 21MT-1 cells after 9 and 15 days growth in 3D Matrigel. (a) Proliferation was quantified by Ki67 immunohistochemical staining of Matrigel plugs. 21PTci cells showed a modest proliferative activity at day 9, which trailed off by day 15. 21NTci cells showed an initial burst of proliferative activity at day 9, which decreased significantly ( $P < 0.01$ ) by day 15. 21MT-1 cells showed a modest proliferative activity that was higher by day 15. (b) Apoptosis was quantified by caspase 3 immunohistochemical staining of Matrigel plugs. At day 9, there were no significant differences in apoptotic rates among cell lines. At day 15, apoptotic rates of both 21PTci and 21MT-1 cells decreased slightly (non significantly and significantly ( $P < 0.05$ ), respectively). (c) When the ratio of proliferation/apoptosis was calculated, 21PTci cells showed a modest cell division over cell death ratio at day 9, which trended toward a decreased ratio at day 15, at which time there was evidence of differentiation in terms of extracellular lumen formation and polarized groups (c.f. Figure 2). 21NTci cells showed an initial burst of proliferative activity over apoptosis at day 9, which decreased significantly ( $P < 0.05$ ) by day 15. 21MT-1 cells showed a modest proliferation/apoptosis ratio at day 9, which significantly increased ( $P < 0.05$ ) at day 15. \*Indicates significance at a level of  $P < 0.05$ .

performed, which identified stage-specific gene alterations. For the 21PTci to 21NTci comparison, 366 probe sets were at least 1.5-fold altered ( $P < 0.05$ ), whereas for the 21NTci to 21MT-1 comparison, 3067 probe sets were at least 1.5-fold up- or downregulated ( $P < 0.05$ ) (data series GSE18370, <http://www.ncbi.nlm.nih.gov/geo/>). To assess whether these alterations would potentially apply to breast cancer progression in a clinical situation (ie, to establish potential clinical relevance), we compared our list of differentially expressed genes with a database we generated from established literature on gene expression profiling of clinical cancer specimens, including papers related to progression,<sup>11–13,49,50</sup> metastasis<sup>45,46,48,49</sup> and prognosis<sup>43,44,47,51</sup> of breast cancer (Supplementary Table 1). Overlap between our initial gene lists (data series GSE18370, <http://www.ncbi.nlm.nih.gov/geo/>) and the clinically relevant databases (Supplementary Table 1) were used to make two more focused genes lists of statistically altered and potentially clinically relevant genes (21PTci to 21NTci: 34 probe IDs; 21NTci to 21MT-1: 227 probe IDs) (Supplementary Table 2). These gene lists were then uploaded into Ingenuity Pathways Analysis (IPA) for further analysis, which identified representation of several major functional and canonical categories (data not shown). Gene lists were then pared down to all genes found within the top 10 functional categories and canonical pathways (21PTci

to 21NTci: 20 genes; 21NTci to 21MT-1: 66 genes) and the gene function as described by GeneCards ([www.genecards.org](http://www.genecards.org)) was recorded (Supplementary Table 3). Based on gene function as described by GeneCards, 19 representative genes between the two transitions were chosen for qRT-PCR validation, with 2 genes (DCN, WNT5A) represented in both transitions (Table 2). If a gene was significantly different ( $P < 0.05$ ) between the two cell lines of interest and in the same direction as the microarray, the gene was considered validated. Of the 19 genes, all genes except BAX and MCM4 were validated by qRT-PCR (Table 2). For the 21PTci to 21NTci comparison, differential expression of BAX, DCN, MAX, MCM4, MGA, VANGL1, WISP1 and WNT5A were real-time PCR analyzed. CCL20, CCR1, CDH1, CXCR4, DCN, S100A2, S100A3, SERPINB5, SNAI2, TBX3, TFF2, TNFAIP3 and WNT5A were validated in the 21NTci to 21MT-1 comparison. It is apparent from this analysis that genes associated with the Wnt pathway (eg, WNT5A, VANGL1, WISP1), and control of cell proliferation vs cell death (eg, MAX, MGA), were particularly associated with the 21PTci to 21NTci (ADH vs DCIS) comparison, whereas in the 21NTci to 21MT-1 (DCIS vs IMC) comparison, loss of tumor suppressors (eg, SERPINB5, S100A2), alterations in transcriptional regulators (eg, TBX3, TNFAIP3, SNAI2), chemokines and their receptors (eg, CCL20, CCR1), and

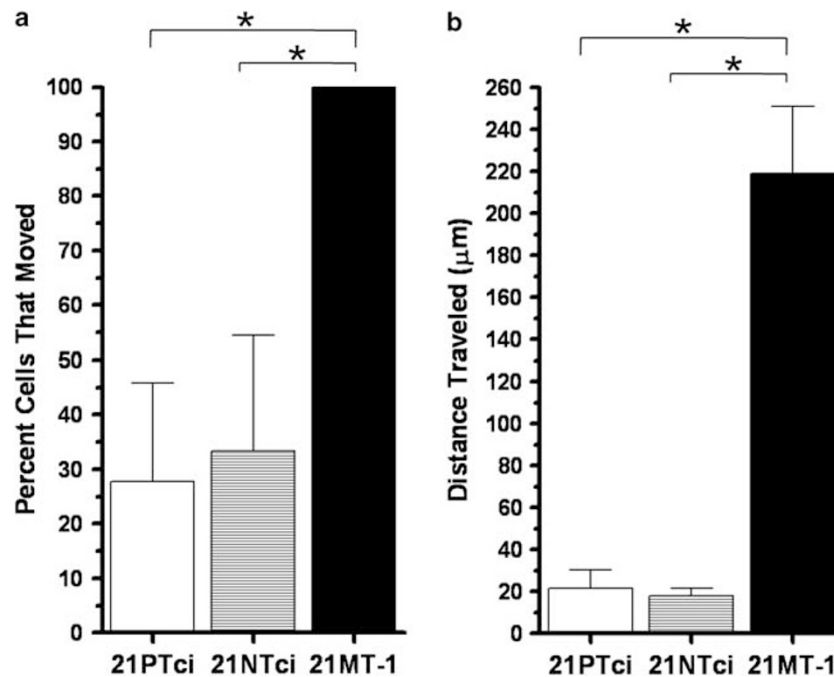


**Figure 4** 21T series cell invasion through Matrigel matrix. Cells were grown in Matrigel for 9 days and then transferred to the incubator stage platform of a time lapse microscope until day 15. Z-stack images were taken every 12 h. All individual cells imaged were followed for the full 6-day interval. (a) Percentage of total cells that moved (invaded) through the Matrigel matrix. A cell was defined as moving if any part of the cell was in a different location compared with the image taken 12 h previously. Here, 100% of 21MT-1 cells showed translational movement, compared with only 27% of 21PTci and 33% 21NTci cells. (b) Distance ( $\mu\text{m}$ ) moving cells traveled through Matrigel matrix. 21MT-1 cells moved significantly further than 21PTci ( $P < 0.01$ ) or 21NTci ( $P < 0.01$ ) cells, which each showed minimal translational movement/invasive ability, consistent with the invasive (21MT-1) vs non-invasive (21PTci, 21NTci) morphologies of these cells when grown *in vivo*. \*Indicates significance at a level of  $P < 0.05$ .

genes associated with motility/invasiveness (eg, TFF2, SERPINB5, S100A2) were identified.

## DISCUSSION

With the institution of mammographic screening programs and advances in breast imaging in recent years, breast cancer is being detected at earlier stages.<sup>52</sup> The liberal use of core biopsies to assess abnormalities detected on imaging has reduced the number of patients inappropriately going to open biopsy when these lesions are benign,<sup>53</sup> but has also increased the number of patients in which potential precursor lesions (such as ADH or DCIS) are detected.<sup>54</sup> When ADH or DCIS are identified on core biopsy, the mainstay of management is surgical excision (with radiotherapy in most cases of DCIS). However, there is little information on the natural biology and progression of these lesions.<sup>55</sup> When there is a chance of residual disease following treatment, options are limited as to further management when the lesions are difficult to detect (eg, lack of associated calcifications) or are widespread. Furthermore, in patients who are genetically predisposed to developing these lesions (such as BRCA1/BRCA2 carriers), management options (short of prophylactic mastectomies) are limited.<sup>56,57</sup> Although there are a few molecularly based systemic options for the management of DCIS either existing or under investigation, (eg, tamoxifen for ER-positive DCIS, trastuzumab for

HER2-positive DCIS), a better understanding of the molecular basis of progression is needed to develop further targeted therapy for these early lesions.<sup>58</sup>

Information from clinical studies examining pre-invasive lesions vs invasive mammary carcinoma has yielded abundant gene expression profile differences between stages of progression (ADH vs DCIS vs IMC) (eg, 11–13,49,50). What is lacking is the understanding of which of these differentially expressed genes may be key players regulating transition through the stages of breast progression, not only to predict which of the lesions are more likely to progress, but to provide potential novel targets for preventative therapies. Unfortunately, few *in vivo* and *in vitro* model systems exist that would allow individual candidate genes to be tested for their influence on human breast cancer progression, or to allow for efficient screening of the many candidate genes of interest. One such system, the HMT-3522 human breast epithelial cell series, has been described and used to identify specific matrix metalloproteinases required for the invasive phenotype.<sup>59</sup> A major advantage of such a system, wherein all of the representative cell lines are derived from the same patient, is that variability related to the individual's genetic background is eliminated (a common problem in comparing across cell lines of differing patient origin). The system we describe here has all the same advantages, and has a further advantage of representation of an even earlier stage,



**Table 2 qRT-PCR validated genes of interest showing significant differences between 21T series cell lines that are of potential clinical relevance<sup>a</sup> and are of the top 10 functional and canonical pathways represented (Ingenuity)**

Common name <sup>b</sup>	Gene name	GeneCard function	Microarray fold change	qRT-PCR fold change <sup>c</sup>
<i>21PTci to 21NTci</i>				
BAX	BCL2-associated X protein	Accelerates programmed cell death	-1.75	1.03
DCN	Decorin	Affects rate of fibrils formation	7.52	6.38
MAX	MYC-associated factor X	Transcription regulator	-1.54	-1.38
MCM4	Minichromosome maintenance complex 4	Involved in control of DNA replication	-1.56	1.14
MGA	MAX gene associated	Transcription regulator	3.23	2.75
VANGL1	Vang-like 1	Planar cell polarity signaling molecule	2.19	1.60
WISP1	WNT1 inducible signal pathway protein 1	Downstream regulator in the Wnt/Frizzled-signaling pathway	2.18	2.15
WNT5A	Wingless-type MMTV integration site family, member 5A	Ligand for members of frizzled family	-1.89	-1.61
<i>21NTci to 21MT-1</i>				
CCL20	Chemokine (C-C motif) ligand 20	Chemotactic factor	19.98	10.90
CCR1	Chemokine receptor 1	Receptor for C-C type chemokine	7.85	4.10
CDH1	Cadherin 1, type 1, E-cadherin	Promotes non-amyloidogenic degradation	-59.88	-2.31
CXCR4	Chemokine (C-X-C motif) receptor 4	Receptor for the C-X-C chemokine CXCL12/SDF-1	-3.81	-33.33
DCN	Decorin	Affects rate of fibrils formation	33.94	72.51
S100A2	S100 calcium-binding protein 2	Has a role in suppressing tumor cell growth	-1.59	-3.02
S100A3	S100 calcium-binding protein 3	Involved in calcium-dependent cuticle cell differentiation	3.67	6.44
SERPINB5	Maspin	Tumor suppressor, blocks growth, invasion and metastatic properties of mammary tumors	-31.33	-47.20
SNAI2	Snail homolog 2, Slug	Transcriptional repressor	2.93	33.58
TBX3	T-box 3	Transcription repressor involved in developmental processes	2.84	2.70
TFF2	Trefoil factor 2	Inhibits gastrointestinal motility	9.71	6.80
TNFAIP3	Tumor necrosis factor, alpha-induced protein 3	Inhibitor of programmed cell death	3.94	2.31
WNT5A	Wingless-type MMTV integration site family, member 5A	Ligand for members of frizzled family	9.30	9.34

<sup>a</sup>Genes found on clinical databases created from the literature.<sup>11-13,43-51</sup>

<sup>b</sup>Nineteen genes are a subset of a larger list (Supplementary Table 3) and have been further assessed by quantitative real-time (qRT-PCR).

<sup>c</sup>Seventeen genes (not BAX and MCM4) validating the microarray data.

pre-DCIS (ADH-like) phenotype (as we described for the 21PTci cells).

We found the 21PT-derived cell line 21PTci to be consistently non-tumorigenic and non-metastatic after injection into the mammary fat pads of nude mice, confirming previous work.<sup>36</sup> However, upon histological examination of the mammary fat pad of these mice, we found occasional lesions mimicking that of ADH. Features consistent with ADH were the mixture of two epithelial cell populations within a given duct, one normal-appearing, the other atypical (and non-high grade), with the atypical cell population represented over an area of <2.0 mm.<sup>2-5</sup> Interestingly, when these cells were grown in 3D Matrigel, they were capable of

forming large numbers of well-defined tubular/acinar structures, with maintenance of cell polarity in the vast majority of the groups. Furthermore, many of these groups showed a mixture of cells with normal-appearing and more atypical nuclei. Proliferative and apoptosis rates were low and cell movement was largely restricted to collective organization within these groups.

In contrast, we found the 21NT-derived cells to be tumorigenic and non-metastatic in those mice that did form lesions (tumor take in about 20%), as described by Band *et al.*<sup>36</sup> Although tumorigenic, we found that the majority of mice in which lesions formed showed a histology representative of DCIS, with no associated invasion. The

involved ducts showed a uniform neoplastic cell population, with intermediate and high grade nuclei, solid and cribriform architectural patterns, with zonal necrosis. Only 1/7 of the injected animals that formed lesions showed an associated invasive component, which was localized to the fat pad, with no evidence of locoregional lymph node involvement or distant metastases. This cell line thus represents a good model of DCIS, in that although in most injected animals it maintains morphology of DCIS only, it does show the potential for a low rate of spontaneous progression to invasive ability. The phenotype is similar to that described for MCF10DCIS cells,<sup>60</sup> although in contrast to MCF10DCIS, 21NT cells are not ras-transformed (a rare event in spontaneous human breast cancer), and show a more stable (less 'leaky') DCIS phenotype than MCF10DCIS cells, which have a higher propensity for invasion with time *in vivo*.<sup>17</sup> When 21NTci cells are grown in 3D Matrigel, features consistent with DCIS-like behavior including the tendency of the cells to arrange into groups, but with poor polarization of the constituent cells, nuclear atypia in all the constituent cells, the spherical, non-infiltrative nature of colonies that formed, and a lack of translational invasive behavior when followed by time lapse microscopy were observed.

The 21MT-1 cells, as described by Band *et al*,<sup>36</sup> were found to be tumorigenic (in the majority of orthotopically injected mice), and metastatic in half the mice that formed primary tumors. Upon histological examination, we found that all of the mice that formed tumors showed invasive mammary carcinoma (no special type, SBR grade III/III), most with admixed DCIS of intermediate and high nuclear grade in the background. Consistent with this *in vivo* phenotype, when the cells were grown in 3D Matrigel, they formed more disorganized, non-spherical colonies, less polarization or lumen formation of cell groups, more single cells, and a much greater ability to show translational movement through Matrigel upon time-lapse microscopy, when compared with the other two cell lines.

We have identified unique differential gene expression profiles for each of the 21T series cell lines, grown in Matrigel. Interestingly, of those genes with evidence for clinical relevance, Wnt pathway alterations (eg, WNT5A, VANGL1, WISP1) are particularly predominant in the comparison between 21PTci and 21NTci (representing the ADH to DCIS transition). This is consistent with recent studies implicating both the canonical and noncanonical Wnt-signaling pathways in initiation and maintenance of breast tumorigenesis (reviewed in Mohinta *et al*<sup>61</sup>) as well as in cancer stem cell self renewal and the initiation of the epithelial to mesenchymal transition.<sup>62</sup> In particular, the planar cell polarity (PCP) pathway (a non-canonical Wnt pathway), involving ligand WNT5A, has been said to have either inhibitory or promoting roles in various cancers, depending on the context (reviewed in Kikuchi and Yamamoto<sup>63</sup>). It has been suggested that early in progression, the PCP pathway functions mainly in an inhibitory role by downregulating canonical Wnt sig-

naling (through  $\beta$ -catenin), and promoting differentiation, whereas later in progression, the PCP pathway may promote progression, by stimulating cell migration and invasion.<sup>64</sup> In the 21T series cell lines, WNT5A is downregulated between 21PTci and 21NTci (ADH to DCIS), and is upregulated between 21NTci and 21MT-1 (DCIS to IMC), in keeping with an early suppressive role and a later promoting role on progression.

Also prominent among genes differentially expressed between 21PTci and 21NTci were genes associated with signaling processes potentially involved with control of cell growth *vs* apoptosis (eg, MAX, MGA). Such changes, resulting in a net increase in cell growth (*vs* apoptosis), would be consistent with the morphological transition from ADH to DCIS, where the neoplastic cell population is seen to expand from partially, to completely filling duct cross-sections. In the comparison between 21NTci (DCIS-like) and 21MT-1 (IMC-like), which focuses on progression to an invasive and metastatic phenotype, differentially expressed genes of potential clinical relevance included the loss of tumor suppressors (eg, SERPINB5, S100A2), alterations in transcriptional regulators believed to be involved in regulating cell senescence/apoptosis (eg, TBX3, TNFAIP3) and promoting invasiveness and epithelial to mesenchymal transition (EMT) (eg, SNAI2), certain chemokines and their receptors (eg, CCL20, CCR1), and genes more directly associated with motility/invasiveness (eg, TFF2, SERPINB5, S100A2). Collectively, these alterations would be expected to increase the malignancy of breast cancer cells, allowing for invasive and metastatic phenotypes to emerge in the DCIS to IMC transition.

The advantages of the approach we have taken in these 21T cell comparisons are two-fold. First, by using a filter for genes showing altered expression in published clinical literature on early breast cancer progression, invasion/metastasis and prognosis, we have narrowed our initial search to genes with potential relevance in a clinical setting. This is not to say that genes showing altered expression that did not 'make' this list are irrelevant, but simply allows us to focus our search to those with some existing support for clinical import. Second, the use of the 21T model provides us with a manipulatable *in vitro* and *in vivo* system for future studies to test the relative functional impact of specific genes on transitions between these early stages of breast cancer progression (ADH to DCIS to IMC). We expect that use of this system will provide an important tool to unlocking some of the intricacies of the molecular influences on early breast progression. The information gathered will be critical to our ability to target and prevent this process and effectively stop breast cancer not just 'in its tracks', but 'before it makes tracks'.

Supplementary Information accompanies the paper on the Laboratory Investigation website (<http://www.laboratoryinvestigation.org>)

#### ACKNOWLEDGEMENTS

We thank David Dales for technical assistance and Larry Stitt for statistical advice. This research was funded by Grant no. 42511 from the Canadian

Institute for Health Research and Grant no. 016506 from the Canadian Breast Cancer Research Alliance with special funding support from the Canadian Breast Cancer Foundation and the Cancer Research Society. LHS is the recipient of a Translational Breast Cancer Studentship from the London Regional Cancer Program. HSL is the recipient of a Canadian Breast Cancer Foundation Post Doctoral Fellowship award. AFC is a Cancer Research Chair in Oncology and receives salary support from the Canada Research Chairs Program.

#### DISCLOSURE/CONFLICT OF INTEREST

The authors declare no conflict of interest.

- Lakhani SR, Collins N, Stratton MR, *et al*. Atypical ductal hyperplasia of the breast: Clonal proliferation with loss of heterozygosity on chromosomes 16q and 17p. *J Clin Pathol* 1995;48:611–615.
- Page DL, Dupont WD, Rogers LW, *et al*. Atypical hyperplastic lesions of the female breast. A long-term follow-up study. *Cancer* 1985;55:2698–2708.
- Page DL, Dupont WD. Anatomic indicators (histologic and cytologic) of increased breast cancer risk. *Breast Cancer Res Treat* 1993;28:157–166.
- Allred DC, Mohsin SK, Fuqua SA. Histological and biological evolution of human premalignant breast disease. *Endocr Relat Cancer* 2001; 8:47–61.
- Arpino G, Laucirica R, Elledge RM. Premalignant and *in situ* breast disease: biology and clinical implications. *Ann Intern Med* 2005;143:446–457.
- Allred DC, Wu Y, Mao S, *et al*. Ductal carcinoma *in situ* and the emergence of diversity during breast cancer evolution. *Clin Cancer Res* 2008;14:370–378.
- Polyak K. Is breast tumor progression really linear? *Clin Cancer Res* 2008;14:339–341.
- Sgroi DC, Teng S, Robinson G, *et al*. *In vivo* gene expression profile analysis of human breast cancer progression. *Cancer Res* 1999;59:5656–5661.
- Worsham MJ, Pals G, Raju U, *et al*. Establishing a molecular continuum in breast cancer DNA microarrays and benign breast disease. *Cytometry* 2002;47:56–59.
- Li Z, Tsimelzon A, Immaneni A, *et al*. A cDNA microarray study comparing noninvasive and invasive human breast cancer. *Proc Am Assoc Cancer Res* 2002;43:901–902.
- Ma XJ, Salunga R, Tuggle JT, *et al*. Gene expression profiles of human breast cancer progression. *Proc Natl Acad Sci USA* 2003;100: 5974–5979.
- Abba MC, Drake JA, Hawkins KA, *et al*. Transcriptomic changes in human breast cancer progression as determined by serial analysis of gene expression. *Breast Cancer Res* 2004;6:R499–R513.
- Schuetz CS, Bonin M, Clare SE, *et al*. Progression-specific genes identified by expression profiling of matched ductal carcinomas *in situ* and invasive breast tumors, combining laser capture microdissection and oligonucleotide microarray analysis. *Cancer Res* 2006;66: 5278–5286.
- Medina D. The preneoplastic phenotype in murine mammary tumorigenesis. *J Mammary Gland Biol Neoplasia* 2000;5:393–407.
- Cardiff RD, Moghanaki D, Jensen RA. Genetically engineered mouse models of mammary intraepithelial neoplasia. *J Mammary Gland Biol Neoplasia* 2000;5:421–437.
- Weaver VM, Howlett AR, Langton-Webster B, *et al*. The development of a functionally relevant cell culture model of progressive human breast cancer. *Semin Cancer Biol* 1995;6:175–184.
- Miller FR. Xenograft models of premalignant breast disease. *J Mammary Gland Biol Neoplasia* 2000;5:379–391.
- Stampfer MR, Yaswen P. Culture models of human mammary epithelial cell transformation. *J Mammary Gland Biol Neoplasia* 2000;5:365–378.
- Santner SJ, Dawson PJ, Tait L, *et al*. Malignant MCF10CA1 cell lines derived from premalignant human breast epithelial MCF10AT cells. *Breast Cancer Res Treat* 2001;65:101–110.
- Briand P, Lykkesfeldt AE. An *in vitro* model of human breast carcinogenesis: epigenetic aspects. *Breast Cancer Res Treat* 2001;65:179–187.
- Fauquette W, Dong-Le Bourhis X, Delannoy-Courdent A, *et al*. Characterization of morphogenetic and invasive abilities of human mammary epithelial cells: Correlation with variations of urokinase-type plasminogen activator activity and type-1 plasminogen activator inhibitor level. *Biol Cell* 1997;89:453–465.
- Weaver VM, Petersen OW, Wang F, *et al*. Reversion of the malignant phenotype of human breast cells in three-dimensional culture and *in vivo* by integrin blocking antibodies. *J Cell Biol* 1997;137:231–245.
- Wang F, Weaver VM, Petersen OW, *et al*. Reciprocal interactions between beta1-integrin and epidermal growth factor receptor in three-dimensional basement membrane breast cultures: a different perspective in epithelial biology. *Proc Natl Acad Sci USA* 1998;95:14821–14826.
- Meiners S, Brinkmann V, Naundorf H, *et al*. Role of morphogenetic factors in metastasis of mammary carcinoma cells. *Oncogene* 1998;16:9–20.
- Benton G, Crooke E, George J. Laminin-1 induces E-cadherin expression in 3-dimensional cultured breast cancer cells by inhibiting DNA methyltransferase 1 and reversing promoter methylation status. *FASEB J* 2009;23:3884–3895.
- Wang X, Zhang X, Sun L, *et al*. Preadipocytes stimulate ductal morphogenesis and functional differentiation of human mammary epithelial cells in 3D silk scaffolds. *Tissue Eng Part A* 2009;15: 3087–3098.
- Shaw KR, Wrobel CN, Brugge JS. Use of three-dimensional basement membrane cultures to model oncogene-induced changes in mammary epithelial morphogenesis. *J Mammary Gland Biol Neoplasia* 2004;9:297–310.
- Hirai Y, Lochter A, Galosy S, *et al*. Epimorphin functions as a key morphoregulator for mammary epithelial cells. *J Cell Biol* 1998;140:159–169.
- Soriano JV, Pepper MS, Orci L, *et al*. Roles of hepatocyte growth factor/scatter factor and transforming growth factor-beta1 in mammary gland ductal morphogenesis. *J Mammary Gland Biol Neoplasia* 1998;3:133–150.
- Simian M, Hirai Y, Navre M, *et al*. The interplay of matrix metalloproteinases, morphogens and growth factors is necessary for branching of mammary epithelial cells. *Development* 2001;128:3117–3131.
- Niemann C, Brinkmann V, Birchmeier W. Hepatocyte growth factor and neuregulin in mammary gland cell morphogenesis. *Adv Exp Med Biol* 2000;480:9–18.
- Ball EM, Risbridger GP. Activins as regulators of branching morphogenesis. *Dev Biol* 2001;238:1–12.
- Debnath J, Mills KR, Collins NL, *et al*. The role of apoptosis in creating and maintaining luminal space within normal and oncogene-expressing mammary acini. *Cell* 2002;111:29–40.
- Debnath J, Brugge JS. Modelling glandular epithelial cancers in three-dimensional cultures. *Nat Rev Cancer* 2005;5:675–688.
- Hebner C, Weaver VM, Debnath J. Modeling morphogenesis and oncogenesis in three-dimensional breast epithelial cultures. *Annu Rev Pathol* 2008;3:313–339.
- Band V, Zajchowski D, Swisshelm K, *et al*. Tumor progression in four mammary epithelial cell lines derived from the same patient. *Cancer Res* 1990;50:7351–7357.
- Biswas DK, Averboukh L, Sheng S, *et al*. Classification of breast cancer cells on the basis of a functional assay for estrogen receptor. *Mol Med* 1998;4:454–467.
- Biswas DK, Cruz A, Pettit N, *et al*. A therapeutic target for hormone-independent estrogen receptor-positive breast cancers. *Mol Med* 2001;7:59–67.
- Cook AC, Tuck AB, McCarthy S, *et al*. Osteopontin induces multiple changes in gene expression that reflect the six 'hallmarks of cancer' in a model of breast cancer progression. *Mol Carcinog* 2005;43: 225–236.
- Tuck AB, Arsenault DM, O'Malley FP, *et al*. Osteopontin induces increased invasiveness and plasminogen activator expression of human mammary epithelial cells. *Oncogene* 1999;18:4237–4246.
- Furger KA, Allan AL, Wilson SM, *et al*. Beta(3) integrin expression increases breast carcinoma cell responsiveness to the malignancy-enhancing effects of osteopontin. *Mol Cancer Res* 2003;1:810–819.
- Luzzi KJ, MacDonald IC, Schmidt EE, *et al*. Multistep nature of metastatic inefficiency: dormancy of solitary cells after successful extravasation and limited survival of early micrometastases. *Am J Pathol* 1998;153:865–873.

43. Asaka S, Fujimoto T, Akaishi J, *et al*. Genetic prognostic index influences patient outcome for node-positive breast cancer. *Surg Today* 2006;36:793–801.
44. O'Brien N, O'Donovan N, Foley D, *et al*. Use of a panel of novel genes for differentiating breast cancer from non-breast tissues. *Tumour Biol* 2008;28:312–317.
45. Minn AJ, Kang Y, Serganova I, *et al*. Distinct organ-specific metastatic potential of individual breast cancer cells and primary tumors. *J Clin Invest* 2005;115:44–55.
46. Kang Y, Siegel PM, Shu W, *et al*. A multigenic program mediating breast cancer metastasis to bone. *Cancer Cell* 2003;3:537–549.
47. Shen R, Ghosh D, Chinnaiyan AM. Prognostic meta-signature of breast cancer developed by two-stage mixture modeling of microarray data. *BMC Genomics* 2004;5:94.
48. Wang Y, Klijn JG, Zhang Y, *et al*. Gene-expression profiles to predict distant metastasis of lymph-node-negative primary breast cancer. *Lancet* 2005;365:671–679.
49. Nishidate T, Katagiri T, Lin ML, *et al*. Genome-wide gene-expression profiles of breast-cancer cells purified with laser microbeam microdissection: Identification of genes associated with progression and metastasis. *Int J Oncol* 2004;25:797–819.
50. Milovanovic T, Planutis K, Nguyen A, *et al*. Expression of wnt genes and frizzled 1 and 2 receptors in normal breast epithelium and infiltrating breast carcinoma. *Int J Oncol* 2004;25:1337–1342.
51. van 't Veer LJ, Dai H, van de Vijver MJ, *et al*. Gene expression profiling predicts clinical outcome of breast cancer. *Nature* 2002;415:530–536.
52. Duffy SW, Agbaje O, Tabar L, *et al*. Overdiagnosis and overtreatment of breast cancer: Estimates of overdiagnosis from two trials of mammographic screening for breast cancer. *Breast Cancer Res* 2005;7:258–265.
53. El-Sayed ME, Rakha EA, Reed J, *et al*. Predictive value of needle core biopsy diagnoses of lesions of uncertain malignant potential (B3) in abnormalities detected by mammographic screening. *Histopathology* 2008;53:650–657.
54. Provenzano E, Pinder SE. Pre-operative diagnosis of breast cancer in screening: Problems and pitfalls. *Pathology* 2009;41:3–17.
55. Simpson JF. Update on atypical epithelial hyperplasia and ductal carcinoma *in situ*. *Pathology* 2009;41:36–39.
56. Kauff ND, Brogi E, Scheuer L, *et al*. Epithelial lesions in prophylactic mastectomy specimens from women with BRCA mutations. *Cancer* 2003;97:1601–1608.
57. Isern AE, Loman N, Malina J, *et al*. Histopathological findings and follow-up after prophylactic mastectomy and immediate breast reconstruction in 100 women from families with hereditary breast cancer. *Eur J Surg Oncol* 2008;34:1148–1154.
58. Boughy JC, Gonzalez RJ, Bonner E, *et al*. Current treatment and clinical trial developments for ductal carcinoma *in situ* of the breast. *Oncologist* 2007;12:1276–1287.
59. Rizki A, Weaver VM, Lee SY, *et al*. A human breast cell model of preinvasive to invasive transition. *Cancer Res* 2008;68:1378–1387.
60. Dawson PJ, Wolman SR, Tait L, *et al*. MCF10AT: A model for the evolution of cancer from proliferative breast disease. *Am J Pathol* 1996;148:313–319.
61. Mohinta S, Wu H, Chaurasia P, *et al*. Wnt pathway and breast cancer. *Front Biosci* 2007;12:4020–4033.
62. DiMeo TA, Anderson K, Phadke P, *et al*. A novel lung metastasis signature links wnt signaling with cancer cell self-renewal and epithelial-mesenchymal transition in basal-like breast cancer. *Cancer Res* 2009;69:5364–5373.
63. Kikuchi A, Yamamoto H. Tumor formation due to abnormalities in the beta-catenin-independent pathway of wnt signaling. *Cancer Sci* 2008;99:202–208.
64. Wang Y. Wnt/Planar cell polarity signaling: a new paradigm for cancer therapy. *Mol Cancer Ther* 2009;8:2103–2109.